

# Photobiomodulation in 3D tissue engineering

Polina Bikmulina<sup>1b</sup>,<sup>a,\*</sup> Nastasia Kosheleva<sup>1b</sup>,<sup>b,c,d</sup> Anastasia Shpichka,<sup>b,d</sup>  
 Vladimir Yusupov<sup>1b</sup>,<sup>e</sup> Vladimir Gogvadze,<sup>f,g</sup> Yury Rochev,<sup>h</sup>  
 and Peter Timashev<sup>1b</sup>,<sup>d</sup>

<sup>a</sup>Sechenov First Moscow State Medical University, World-Class Research Center  
 “Digital Biodesign and Personalized Healthcare”, Moscow, Russia

<sup>b</sup>Sechenov First Moscow State Medical University, Institute for Regenerative Medicine,  
 Moscow, Russia

<sup>c</sup>FSBSI Institute of General Pathology and Pathophysiology, Moscow, Russia

<sup>d</sup>Sechenov University, Laboratory of Clinical Smart Nanotechnologies, Moscow, Russia

<sup>e</sup>Institute of Photon Technologies of FSRC “Crystallography and Photonics” RAS,  
 Troitsk, Russia

<sup>f</sup>Lomonosov Moscow State University, Faculty of Medicine, Moscow, Russia

<sup>g</sup>Karolinska Institutet, Institute of Environmental Medicine, Division of Toxicology,  
 Stockholm, Sweden

<sup>h</sup>National University of Ireland, Galway, Galway, Ireland

## Abstract

**Significance:** The method of photobiomodulation (PBM) has been used in medicine for a long time to promote anti-inflammation and pain-resolving processes in different organs and tissues. PBM triggers numerous cellular pathways including stimulation of the mitochondrial respiratory chain, alteration of the cytoskeleton, cell death prevention, increasing proliferative activity, and directing cell differentiation. The most effective wavelengths for PBM are found within the optical window (750 to 1100 nm), in which light can permeate tissues and other water-containing structures to depths of up to a few cm. PBM already finds its applications in the developing fields of tissue engineering and regenerative medicine. However, the diversity of three-dimensional (3D) systems, irradiation sources, and protocols intricate the PBM applications.

**Aim:** We aim to discuss the PBM and 3D tissue engineered constructs to define the fields of interest for PBM applications in tissue engineering.

**Approach:** First, we provide a brief overview of PBM and the timeline of its development. Then, we discuss the optical properties of 3D cultivation systems and important points of light dosimetry. Finally, we analyze the cellular pathways induced by PBM and outcomes observed in various 3D tissue-engineered constructs: hydrogels, scaffolds, spheroids, cell sheets, bioprinted structures, and organoids.

**Results:** Our summarized results demonstrate the great potential of PBM in the stimulation of the cell survival and viability in 3D conditions. The strategies to achieve different cell physiology states with particular PBM parameters are outlined.

**Conclusions:** PBM has already proved itself as a convenient and effective tool to prevent drastic cellular events in the stress conditions. Because of the poor viability of cells in scaffolds and the convenience of PBM devices, 3D tissue engineering is a perspective field for PBM applications.

© The Authors. Published by SPIE under a Creative Commons Attribution 4.0 International License. Distribution or reproduction of this work in whole or in part requires full attribution of the original publication, including its DOI. [DOI: [10.1117/1.JBO.27.9.090901](https://doi.org/10.1117/1.JBO.27.9.090901)]

**Keywords:** photobiomodulation; tissue engineering; regenerative medicine; low-level light.

Paper 220027VRR received Feb. 4, 2022; accepted for publication Aug. 28, 2022; published online Sep. 14, 2022.

\*Address all correspondence to Polina Bikmulina, [bikmulina\\_p\\_yu@staff.sechenov.ru](mailto:bikmulina_p_yu@staff.sechenov.ru)

## 1 Introduction

Photobiomodulation (PBM) is a nonthermal process that utilizes nonionizing forms of light sources, including lasers, LEDs, and broadband light in the visible (400 to 750 nm) and infrared range (750 to 1100 nm).<sup>1,2</sup> The process of PBM of biological objects is usually referred to as an irradiation.<sup>3-5</sup> Historically, the PBM application in clinics began earlier than any clinical trials, *in vivo* or *in vitro* tests on this method. The PBM effects themselves were first discovered in 1967 by Endre Mester while he was trying to treat an advanced melanoma in one of his patients.<sup>6</sup> Intrigued by the results of laser irradiation being opposite to those expected, Mester continued his experiments on mice—and his works are the first known confirmation of the PBM effects.<sup>7</sup> Nowadays, PBM is widely utilized for various clinical and therapeutic applications. PBM in the red and NIR ranges have proven itself to be beneficial for the repair of cartilage and bone defects,<sup>8,9</sup> a wide range of neuronal disorders,<sup>10</sup> and is also capable of resolving pain, decreasing inflammation, and accelerating healing.<sup>11-13</sup> Currently, there are more than 600 registered clinical trials related to PBM, and more than half of them have been successfully completed. The trials based on the PBM include various conditions, such as postoperative wounds, chronic pain, skin diseases, and more (details are provided in Table 1). Based on this clinical research, PBM devices using both lasers and LEDs have been cleared for marketing by FDA.<sup>14-16</sup>

The use of PBM in clinical practice was followed by gradual understanding of its mechanisms. Cytochrome C oxidase (CCO) is considered the main target of red and NIR light in a cell. PBM can influence on oxidative processes in cells, ATP production, calcium waves, and other processes associated with the mitochondria metabolism. The second messengers, such as NO, ATP, ROS, and Ca<sup>2+</sup>, are activated via the redox changes of the mitochondrial electron transport chain.<sup>17,18</sup> This leads to the upregulation of various cellular pathways, linked to cell proliferation, differentiation, metabolic changes, antiapoptotic, or anti-inflammatory effects.<sup>19</sup> With developing methods of cell biology, a deeper understanding of the PBM effects and mechanisms

**Table 1** Completed clinical trials on PBM.

Number	Number of patients	Condition/disease	Results
NCT02383472	53	Mild traumatic brain injury	Positive effects on verbal and visual memory, decreased reaction time, increased visual motor speed
NCT01439724	94	Oral mucositis on the background of chemotherapy	Decreased morbidity, prevention of the oral mucositis relapses
NCT02267850	29	Orthodontic treatment time	Accelerated tooth movement
NCT02181400	21	Diabetic macular oedema	Anatomical improvement of macular oedema
NCT03741062	11	Wound healing of human palatal tissue	Improved wound healing and postoperative comfort, prevention of scars, decreased consumption of analgesic pills
NCT00929773	100	Chronic pain in neck and shoulders	Increased range of motion, decreased reported degree of pain
NCT01821352	53	Obesity	Reduction of circumference of hips, waist, and upper abdomen
NCT02588599	54	Toenail onychomycosis	Increased extent of clear nail
NCT01538199	28	Major depressive disorder	Reduced posttreatment depression ratings

becomes possible. Moreover, the upcoming fields of regenerative medicine and, in particular, tissue engineering (TE), provide a new platform for the PBM application. As mentioned above, the therapeutic range of PBM wavelengths (600 to 1000 nm) is conditioned not only by the cellular susceptibility but also by the light penetration properties. The so-called optical transparency window allows PBM to permeate hydrated tissues, scaffolds, and hydrogels with high efficacy.<sup>20,21</sup> In the last decades, the scope of such 3D cultivation systems' application in the fields of biology and medicine has been constantly expanding. Scaffolds and hydrogels gradually replace classic monolayer cultures when used as drug screening platforms, native tissue models, or clinical products. 3D systems have several crucial advantages over 2D cultures, notwithstanding limitations reducing their applications. Biomaterials with required mechanical properties often can affect cell viability due to the restricted diffusion, mechanical and nutritional stress. Therefore, effective and convenient approaches to maintain the viability of 3D tissue-engineered constructs are of great interest. The PBM technique is noninvasive and does not require direct manipulations of scaffolds or cell media. Light penetrates hydrogels in the range of the most commonly used thicknesses easily. Furthermore, with the development of LED sources and semiconductor lasers (LD, laser diodes), the precise technical characterization of the applied light becomes available. Such LED and LD sources often represent mobile, compact, and controllable devices. These advantages allowed LEDs and LDs to be applied in the upcoming bioprinting approaches. Most of the existing extrusion bioprinters have ultraviolet light sources to perform the photocrosslinking of printed constructs. The practical convenience of these devices should be noted here, because bioprinting requires an accurate dose and duration of irradiation in the conditions of limited space and time. As can be seen from the diversity of both commercial and original extrusion bioprinters, LEDs and LDs match all these demands successfully. Furthermore, the supplementation of a 3D bioprinter with a red or NIR light source for PBM of cells during the printing will cause no technical issues. Several studies have already shown the potential of PBM for a better scaffold's integration in the host tissues,<sup>22</sup> promotion of vascularization,<sup>23</sup> and as a preconditioning method for cell therapy.<sup>24,25</sup>

All these factors make it rational and effective to use red and NIR light with optical transparent scaffolds laden with weakened cells. However, due to the diversity of PBM sources and parameters, cell types, scaffold compositions, and geometries, it is hard to predict whether the chosen combination of factors would be effective or not. In this review, we aim to define the key points regarding PBM of cells in 3D scaffolds for outlining the optimal strategies of PBM application in TE. We first define the main limitations of 3D cell cultivation systems and some PBM properties, which can help to overcome these limitations. Next, we describe the optical properties of tissue-engineered constructs and available sources and parameters of PBM. Finally, we discuss the main mechanisms and cellular pathways triggered by PBM and the following outcomes of PBM of cells in scaffolds to define promising strategies for the cell survival stimulation in 3D scaffolds.

## 2 Tissue-Engineered Constructs: Promises and Limitations

To date, tissue-engineered constructs consisting of scaffolds and cells represent one of the foremost branches of regenerative medicine. 3D cultivation systems offer the *in vivo*-like conditions for cells due to the presence of extracellular matrix (ECM), cell-ECM contacts, mechanical signals, and nutritional and chemical gradients.<sup>26-28</sup> These systems are applicable for native tissue modeling, disease mechanism investigation, drug screening, and cell therapy.<sup>29-35</sup> However, various 3D systems often have drawbacks such as restricted diffusion and lack of vascularization, which can lead to hypoxia, nutritional stress, and cell death.<sup>36,37</sup>

### 2.1 Altered Diffusion of Macromolecules and Oxygen in Tissue-Engineered Constructs

Diffusion coefficients of molecules can vary depending on the diverse scaffold's features. First of all, the molecule size, scaffold-building proteins' concentration, and the rates of cell metabolic activity should be mentioned.<sup>38</sup> The diffusion transport is also defined by the structural

properties of the scaffold, such as the porosity, pore size, overall linear size, tortuosity, microcavities, and geometrical features.<sup>39</sup>

The average diffusion coefficients of dextran in human skin are  $9 \times 10^{-12} \text{ m}^2 \text{ s}^{-1}$  for 500 kDa and  $2.3 \times 10^{-11} \text{ m}^2 \text{ s}^{-1}$  for 40 kDa.<sup>40</sup> As for macroporous scaffolds, the diffusion coefficient of small molecules (oxygen, glucose, calcium, phosphates) is typically around  $10^{-9}$  to  $10^{-10} \text{ m}^2 \text{ s}^{-1}$ , and for the larger ones (molecular weights 4.4 kDa to 2 MDa) it lies in the range of  $10^{-10}$  to  $10^{-11} \text{ m}^2 \text{ s}^{-1}$ .<sup>41-43</sup> As observed in Ref. 38, the diffusion coefficient of oxygen in different biomaterials varies from 0.24 to  $2.5 \times 10^{-9} \text{ m}^2 \text{ s}^{-1}$ , whereas in water it is  $2.7 \times 10^{-9} \text{ m}^2 \text{ s}^{-1}$ . Some studies, however, show that the extracellular matrix does not restrict diffusion of small molecules.<sup>44</sup> According to Ref. 38, the determining factor for the oxygen level inside a construct is not the polymer concentration, but the cell density. The oxygen consumption in a 3D construct is influenced by the monolayer cell culture properties before seeding onto a scaffold. Cells cultured under low confluency consume oxygen rapidly, which causes the oxygen level to drop to almost zero 8 to 10 h after the inoculation.<sup>45</sup>

An appropriate oxygen level is one of the crucial conditions for the normal cell physiology. Usually, cells are cultivated in normoxia (21% oxygen), although the *in vivo* oxygen level is considered to be around 5% to 8%.<sup>46,47</sup> Low oxygen tension has been shown to maintain an active state of stem and progenitor cell populations.<sup>48</sup> On the other hand, the lack of oxygen in a tissue-engineered construct can reduce the cell viability.<sup>38,41,49</sup> Typical oxygen diffusion distances in the tissues are restricted to 100 to 150  $\mu\text{m}$ .<sup>50</sup> In case of exceeding this value, after a few days of cultivation, the oxygen levels inside the scaffold drop dramatically, which causes cell death.<sup>51</sup> Some of the authors consider glucose levels and not oxygen the main limiting factor.<sup>52</sup> Average diffusion distances for such metabolites as glucose are in the range between 5 and 200  $\mu\text{m}$ .<sup>50</sup>

The restricted diffusion is aggravated by the lack of vascularization. Cells in a construct can be distanced as far as a few millimeters from the closest capillary, whereas in native tissues these distances do not exceed 20 to 30  $\mu\text{m}$ .<sup>53</sup> In a static culture conditions, parts of tissue-like constructs outlying the surface more than 0.5 to 1 mm contain only dead cells.<sup>54</sup> If the depth of a construct goes beyond 100 to 200  $\mu\text{m}$ , the cell viability drops significantly due to the nutritional stress and oxygen deprivation<sup>55-57</sup> (Fig. 1). Such expansive cell death is considered to be one of the major reasons for transplantation failures.<sup>61,62</sup>

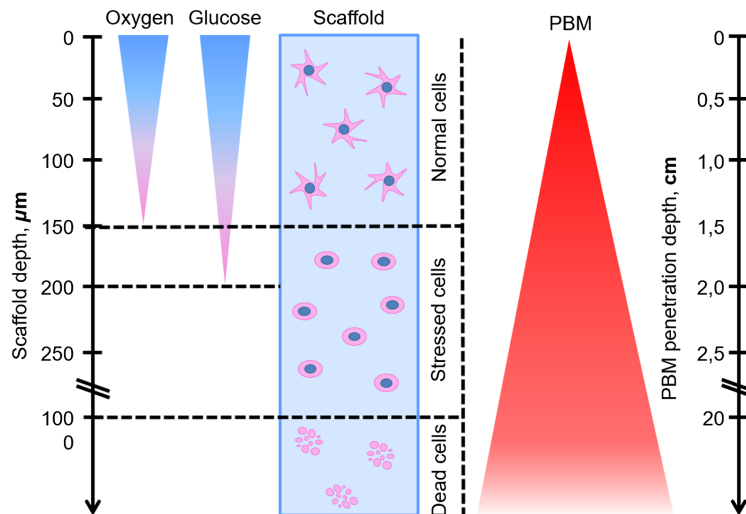


**Fig. 1** Average diffusion distances of oxygen and nutrients (glucose) matched with cell viability on different depths of the scaffold and PBM penetration abilities. The diffusion distance for oxygen is  $\sim 150 \mu\text{m}$ , for glucose is  $200 \mu\text{m}$ . In a range of 0 to  $150 \mu\text{m}$  of scaffold cells are metabolically active and viable.<sup>50</sup> After reaching diffusion limits, cells are exposed to deprivation of oxygen and nutrients. As a result, proliferation, metabolic activity, and general viability decrease. At depths more than 1 mm cell death occurs.<sup>54</sup> Depending on tissue/scaffold and light source type, PBM penetration depth varies from 2 to 3 to 23 cm.<sup>58-60</sup>

## 2.2 Approaches to Stimulate Cell Survival in Tissue-Engineered Constructs

Numerous approaches have been developed to maintain viable 3D cultures. Some of them aim at enhancing the nutrient supplementation via the formation of microchannels, utilization of bioreactors, additional oxygen carriers, hyperbaric oxygen, cocultures of endothelial cells, whereas others stimulate cell growth and survival with growth factor incorporation, hypoxic priming, and preconditioning.<sup>36</sup> Preconditioning usually implies a soft stress (hypoxia, acidic conditions, and nutrient deprivation), which allows cells to adapt to the subsequent unfriendly environment (observed in Ref. 63). Hypoxia stabilizes HIF-1 $\alpha$  (hypoxia-inducible factor-1 $\alpha$ ), which is responsible for cell proliferation, differentiation, migration, survival, glucose adjustment, and vascularization.<sup>64</sup> Some metabolites, such as low concentrations of H<sub>2</sub>O<sub>2</sub> and NO, can be used as preconditioning agents against the oxidative stress.<sup>65,66</sup> Mechanical stimulations—pressure, compression, and exposure to sonic waves—were shown to enhance chondrogenic differentiation.<sup>67</sup> By mimicking the damaged tissue environment, the acidic conditions can stimulate cell survival, migration, and vascularization.<sup>68</sup> Light preconditioning has already been utilized to increase the retinal cells' resistance to the light stress.<sup>69</sup> Moreover, PBM can act as a preconditioning agent for the other stress conditions, such as inflammation or apoptosis.<sup>24,25,70</sup> Due to the involved mechanisms and achieved effects discussed in details below, PBM could be another relatively new method applied for cell preconditioning in 3D systems. Falling in the optical transparency window, the PBM of red and NIR spectrum can surpass the threshold diffusion distances (Fig. 1). Cells in the depths more than 150  $\mu$ m undergo the stress, and therefore can be more susceptible to the PBM.<sup>71,72</sup> Applying light to the 3D scaffolds allows to trigger cell pathways and increase survivability, implant integration, etc. For instance, NIR light successfully applied to promote integration of bone grafts in periodontal areas, skull, and osteoporotic cartilages.<sup>22,73,74</sup> Even more, the vascularization of model 3D hydrogel cultures and spheroids was shown, indicating the PBM ability to provide a functional interaction between implanted graft and host tissues.<sup>23,75,76</sup> PBM is already used in clinical practice to resolve chronic pain and enhance wound healing (Table 1), proving the possibility of PBM devices certification for specific purposes. Therefore, it became clear that PBM might be a promising approach to enhance the viability of cells in a 3D system.

## 3 Photobiomodulation and Scaffolds: Intersection Points

### 3.1 Irradiation Parameters and Light Sources for Photobiomodulation

The biological response to PBM strongly depends on the irradiation parameters, such as the wavelength, intensity (power per unit of irradiated area), and dose (energy per unit of the irradiated area, which can be defined by the intensity multiplied by exposure time).<sup>17,77</sup> The outcome of PBM depends on the wavelength chosen. For instance, wavelengths of 623, 672, 767, and 812 nm were shown to stimulate the DNA synthesis,<sup>78</sup> whereas 915 nm had no effects on the proliferation of the MG63 cell line.<sup>79</sup> The dependence of the PBM effectivity on the intensity or dose can be described by the Arndt–Schultz law of biphasic intensity and the dose response.<sup>80</sup> Cell growth can be enhanced in the narrow range of rather small doses (0.17 J/cm<sup>2</sup>), whereas higher doses usually suppress the cell metabolic activity.<sup>81,82</sup>

The majority of the authors note that PBM effects do not depend on the coherency of the source.<sup>83,84</sup> While it is generally the case that LED devices are considered safer to use than lasers and can be less expensive,<sup>85,86</sup> with the development of electronic devices/semiconductor materials, a wide variety of semiconductor lasers (LD) appeared on the market, which, like LEDs, are cheap, easy to operate, and make it possible to create matrices for irradiating large areas and miniature wearable devices.

### 3.2 Optical Properties of Tissue-Engineered Constructs and Scaffolds

An important feature defining the noninvasive properties of PBM is the transparency window, characterized by the penetration depths (Fig. 2). The penetration depth in tissues and scaffolds can be defined as the light path at which the intensity of the light becomes 1/e of its initial value.

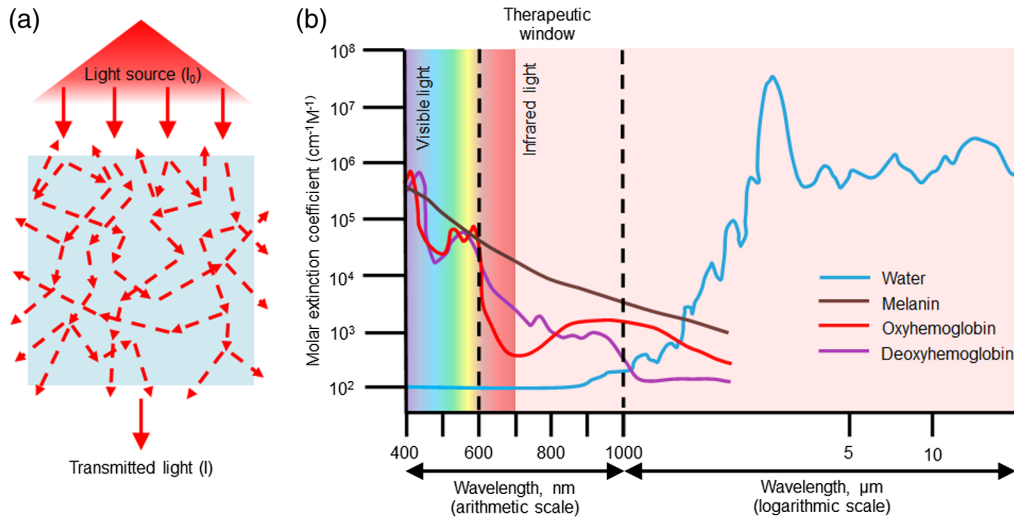


**Fig. 2** (a) the scheme of light transmittance in 3D scaffold systems. Dotted arrows indicate scattering, absorption, and reflection of light. (b) The intersection of water absorption spectrum with the PBM therapeutic wavelengths range. The optical window, where the light absorbance is minimal, is between 600 and 1300 nm. The most spread and effective wavelengths of PBM are in the range of 600 and 1000 nm.

The light with wavelengths between 600 and 1300 nm is only slightly absorbed by water and therefore can penetrate tissues to depths up to a few centimeters.<sup>20,21</sup> The average penetration of transcranial red/NIR light (630 to 810 nm) is up to 70% in mice and up to 10% in humans.<sup>10</sup> The majority of scaffolds (especially hydrogels) are extensively hydrated, and consequently, they are almost transparent in visible and NIR spectral regions. However, light penetration can be significantly impacted by the tissue absorption and scattering, with the degree of reduction depending on wavelength used.<sup>87</sup> Following the tissue architecture and light source parameters, light penetration can be restricted to 10 to 50 mm.<sup>88,89</sup>

Therefore, the exposure level for cells located in a 3D scaffold will be altered due to the light absorption and scattering in the scaffold volume. On average, the light intensity or power density is reduced with the scaffold depth. A strong difference may result in a partial exposure of the cells beyond the “therapeutic range” of PBM. To evaluate this effect, it is important to know the light intensity distribution throughout the entire scaffold’s volume.<sup>90</sup>

The ability of a medium to absorb and scatter photons can be described using an absorption coefficient  $\mu_a$  and a scatter coefficient  $\mu_s$ . These coefficients are defined by the probability that the photon will be absorbed or scattered along the infinitesimal path section  $ds$ . The mean-free path for an absorption event is  $1/\mu_a$ , and the mean-free path for a scattering event is  $1/\mu_s$ .<sup>91</sup> The intensity of the initially collimated beam of light (a thin beam where photons propagate in parallel) is considered to exponentially decrease with the increasing sample depth depending on the Beer–Lambert’s law:

$$I(z) = (1 - R) \cdot I_0 \cdot \exp(-\mu_t z), \quad (1)$$

where  $R = [(n - 1)/(n + 1)]^2$  is the reflection coefficient from the sample surface,  $n$  is the relative average refractive index of the sample and the environment,  $I_0$  is the incident light intensity,  $\mu_t = \mu_a + \mu_s$  is the total attenuation coefficient, and  $z$  is the depth.

Equation (1) represents a single-scattering approximation and is correct when  $\mu_a \gg \mu_s$ . Nevertheless, in tissues and scaffolds, the opposite relationship is observed:  $\mu_s \gg \mu_a$  since scattering significantly predominates over absorption in the visible and NIR spectral regions. In that case, the intensity of a wide laser beam of the incident intensity  $I_0$  at depths  $z > l_d = 1/\mu_{\text{eff}}$  in a thick tissue may be described as

$$I(z) \approx (1 - R) \cdot I_0 \cdot b_s \cdot \exp(-\mu_{\text{eff}} z), \quad (2)$$

where  $\mu_{\text{eff}} = [3\mu_a(\mu_s' + \mu_a)]^{1/2}$  is the effective attenuation coefficient,  $\mu_s' = (1 - g)\mu_s$  is the reduced (transport) scattering coefficient,  $g$  is the scattering anisotropy factor (mean cosine

of the scattering angle), and  $b_s$  accounts for the additional irradiation of the upper layers of a tissue due to backscattering (photon recycling effect).<sup>92</sup>

In real cases, wide laser beams are used for PBM of highly scattering tissues with low absorption. As a result, continuous light energy is accumulated in the tissue due to the high multiplicity of chaotic long-path photon migrations. The light intensity within the superficial zone of the tissue may substantially (up to five times) exceed the incident intensity  $I_0$ .<sup>93</sup> The cells, therefore, are exposed to various doses of PBM depending on their position inside the scaffold. It should also be noted that the intensity distribution within a tissue or scaffold depends not only on the sample's optical properties and the light wavelength but also on the illumination geometry.<sup>94</sup>

However, in the actual case of a biological tissue or scaffold, the light scattering coefficient significantly exceeds the absorption coefficient, and the Beer–Lambert law could not be applied correctly. In this case, a more relevant mathematical description is the diffusion approximation to the radiative transfer equation.<sup>95</sup> The diffusion theory provides a good approximation for small scattering anisotropy factor  $g \leq 0.1$ , whereas for many tissues  $g \approx 0.6$  to  $0.9$  and can be as large as  $0.990$  to  $0.999$  for blood. It should also be noted that the diffusion approximation does not allow one to describe boundary effects. This significantly restricts the applicability of the diffusion approximation.<sup>95</sup>

For modeling photon migration in turbid media, especially in bio-optical imaging applications, the Monte Carlo calculation method can be effective.<sup>95,96</sup> Random migrations of photons inside a sample can be traced from their input until absorption or output occur. Using the given initial and boundary conditions, as well as the known optical characteristics of the material, this method makes it possible to calculate the distributions of light intensity and absorbed energy in samples of polylactide scaffolds and tissues.<sup>90,95,97</sup> Unfortunately, Monte Carlo-based photon migration is significantly limited by the low computational efficiency.

With the growing incident beam diameter,  $I_0$  (initial intensity) increases, leading to higher  $I_z$  (intensity inside the scaffold). Thereby, cells in the volume of the scaffold are irradiated more evenly. Accordingly, light sources with larger apertures are more suitable for medical purposes. Lasers emit a narrow-band monochromatic light with full width at half maximum (FWHM)  $\ll 1$  nm. In that case, a system of lenses or telescopic beam expanders are required for the light beam expansion.<sup>98,99</sup> An LED (nonmonochromatic light with FWHM often in the range of 20 to 50 nm) or LD (monochromatic light with FWHM  $< 3$  nm) are an alternative here. These semiconductor sources usually have a small area ( $< 1$  mm<sup>2</sup>) and LED/LD matrices or integrated optical components may be used to shape its radiation pattern.<sup>100–102</sup> LED and LD matrices are also more efficient for homogeneous irradiation of large areas, but, without special shapers, light intensity from laser devices often has a Gaussian shape with a maximum irradiance at the center and decreased irradiance on the periphery.

It is known that the efficiency of PBM, in addition to other parameters, significantly depends on the wavelength of light.<sup>103,104</sup> In the case of a biological tissue or scaffold, this relation is also superimposed on the wavelength dependence of the distribution of intensity and absorbed energy inside the medium. Therefore, in a real case, the efficiency with which light causes biochemical changes in the volume of biological tissue will significantly depend not only on the illumination (light intensity) on the “input” surface of the object but also on the selected wavelength.

Thus, precisely controlling the PBM parameters is crucial to predict the cell behavior, especially in the presence of a 3D scaffold. Although the majority of hydrogels are optically transparent to red and NIR wavelengths, light scattering can disturb the uniformity of the PBM exposure. In such cases, LED or LD sources are favorable, representing a simple, flexible, and reproducible system for the cell physiology stimulation.

## 4 Cellular Mechanisms of Photobiomodulation

The PBM mechanisms have been investigated for a long time; however, there is still no clear understanding on all the PBM pathways. The reason for that lies in a high variability of applied PBM parameters, biological objects used, and cell environment influencing on light delivery. In general, a long list of PBM targets exists, including cell surface channels and receptors, mitochondrial chromophores, and extracellular enzymes reviewed in Refs. 18 and 72. Targets, such

as transient receptor potential channels, cryptochromes, and opsins, are usually react with light in green and blue spectrum. Antioxidant enzymes, namely glutathione, superoxide dismutase, and catalase, are often present in the tissue extracellular space and can be activated or inhibited in response to PBM to reduce inflammation.<sup>105–107</sup> Here, we focus on the red and NIR PBM mechanisms connected to the mitochondrial chromophores since this pathway represents the most interesting for cells in 3D structures.

#### 4.1 Primary Acceptors of Red and Near Infra-Red Light in a Cell

CCO in the mitochondrial electron transport chain is considered the most essential acceptor of red and NIR light in cells.<sup>18,108</sup> This complex is responsible for the electron transfer from cytochrome c to molecular oxygen and can modulate redox processes in the cell.<sup>18</sup> CCO, or complex IV, contains light-absorbing heme and copper centers.<sup>109–111</sup>

#### 4.2 Secondary Messengers Activated by Light

The initial biochemical processes initiated by red or NIR light relate to CCO itself. In the conditions of the oxidative stress or inflammation, iNOS (inducible NOS, type II NOS) is assembled to produce nitric oxide (NO).<sup>112</sup> NO acts as an antioxidant, controlling free radical levels in the lipid peroxidation processes, relaxes blood vessels' walls, regulates enzymes, induces endothelial cell differentiation and modulates inflammation.<sup>109,113</sup> NO can bind to CCO and reversibly inhibit it, which results in reduced mitochondrial respiration.<sup>114,115</sup> PBM can induce photolysis of the CCO–NO complex, leading to the CCO release and stimulation of the electron transport chain activity<sup>116</sup> followed by the mitochondrial membrane potential increase, which facilitates production of ATP, ROS, and accumulation of  $\text{Ca}^{2+}$ .<sup>108</sup> Moreover, photoproduced NO can take part in the regulation of the cellular pathways.

After the PBM-induced and CCO-mediated stimulation of the mitochondrial electron transport chain, mitochondria can convert more oxygen molecules ( $\text{O}_2$ ) to reactive oxygen species (ROS), such as a superoxide radical ( $\text{O}_2^-$ ).<sup>117–119</sup> High concentrations of ROS are harmful to cells, however, small amounts can regulate the cell physiology.<sup>120</sup>

#### 4.3 Cellular Pathways Triggered by Photobiomodulation

One of the most pronounced metabolic effects of PBM is the increased ATP production.<sup>117</sup> ATP, as a source of energy, maintains the cell metabolism by itself and is also implicated in the protein and DNA synthesis, gene expression, and stimulation of the ERK1/2 pathway. PBM often increases the concentration of intracellular  $\text{Ca}^{2+}$  due to its release from the intracellular stores.<sup>121,122</sup> Intracellular calcium takes part in the cell cycle regulation, cytoskeleton changes, and activation of the cellular pathways, for instance, changes in the  $\text{Ca}^{2+}$  concentration is an important mitogenic signal.<sup>123</sup> NO, ATP,  $\text{Ca}^{2+}$ , and ROS, as secondary messengers, are involved in various cellular pathways, leading to a wide range of downstream effects (summarized in Fig. 3). These effects include increased proliferation (via the MAPK11 cellular pathway), resistance to the oxidative stress, antiapoptotic processes, respiratory chain regulation, and DNA repair.<sup>124</sup>

Many PBM-inducible pathways are related to redox processes and therefore ROS production. NF- $\kappa$ B (nuclear factor kappa B) is one of these; it regulates numerous physiological processes, such as apoptosis, differentiation, proinflammatory genes expression, and responses to the oxidative stress.<sup>125</sup> ROS-dependent NF- $\kappa$ B activation triggers epigenetic mechanisms via histone acetylation.<sup>126</sup> Other pathways activated by changing the redox status include protein kinases, growth factors, chemokines, and more.<sup>127</sup> Activation of ROS-dependent processes is restrained by the level of antioxidants, in particular.<sup>128</sup>

Depending on the PBM parameters, cell type and its redox status, external conditions, and other factors, cells can respond to light in different ways. One of the most frequent effects of PBM is stimulation of proliferation. It has been shown on different cells subjected to various PBM conditions. This effect is wavelength-dependent; stimulation of proliferation was observed only for red and NIR light but not for green and blue light of the same intensity.<sup>117,129</sup> Cell



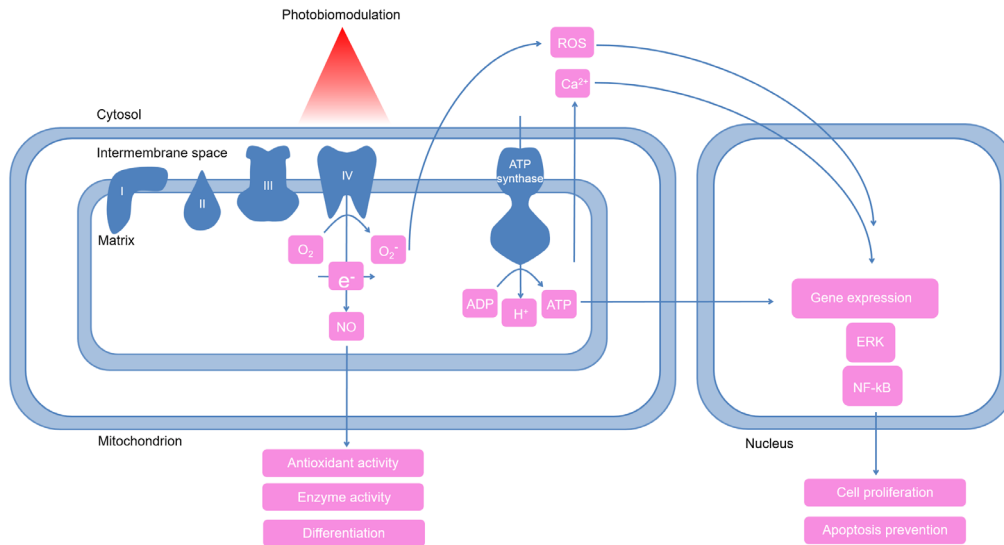


**Fig. 3** Primary events in cells induced by red and NIR light. First, light is absorbed by CCO (unit IV) and as a result, an inhibitory molecule of NO is released.<sup>111</sup> NO can promote endothelial cell differentiation and regulate various enzymes. Moreover, the activity of CCO increases and the transport of electrons within the respiratory chain is stimulated. As a result, more the leakage of electrons increases and oxygen molecules ( $O_2$ ) are converted into superoxide radical ( $O_2^-$ ). Reactive oxygen species can facilitate release of mitochondrial  $Ca^{2+}$  into cytosol.<sup>108</sup> All of these factors, NO, reactive oxygen species, ATP, and  $Ca^{2+}$ , can act together or individually as mediators of cellular pathways and lead to activation of proliferation, cell differentiation, protection of oxidative cell damage, and modulation of apoptosis.

proliferation was driven by PI3K/PKB, PI3K/Akt, Ras/Raf/ERK, PKC, Notch-1 pathway activation or D1, E, and A cyclin expression.<sup>130,131</sup> Usually, these processes are mediated by  $Ca^{2+}$  signaling.

Differentiation is an *in vitro* effect of PBM opposite to proliferation. The most often applied treatment involves a combination of PBM with classical differentiation inducers and results in earlier expression of specific markers.<sup>132,133</sup> The high efficacy of PBM was shown for endothelial differentiation due to the eNOS stimulation and NO formation.<sup>134</sup>

Another beneficial feature of PBM is the ability to inhibit apoptosis, primarily via the modulation of the Bcl-2 and Bax protein expression.<sup>135,136</sup> Besides the biochemical outcomes of PBM, it can be involved in the regulation of the mitochondrial fusion and fission balance. Fusion provides protection from the nutritional and oxidative stress, autophagy, apoptosis, and mitochondrial mutations.<sup>137</sup> Excessive fission or fragmentation can lead to reducing the respiratory activity and is involved in the apoptosis initiation.<sup>138</sup> PBM was shown to increase the expression of MFN2, one of the proteins responsible for mitochondrial fusion.<sup>139</sup>

## 5 PBM for Tissue Engineering and Regenerative Medicine

The first issue to be addressed regarding PBM applications is its variety depending on different types of cells. For instance, human bone marrow-derived mesenchymal stem cells and adipose-derived stem cells (hASCs) respond oppositely to the equal PBM exposure. In the first case, proliferation intensifies, whereas in the second case, cell viability is reduced.<sup>140</sup> The composition and structure of the utilized 3D systems should also be considered when choosing the proper cell type and PBM mode. For example, one should expect the osteogenic differentiation in rigid mineral-containing scaffolds, the neural differentiation in soft hydrogel systems, and the angiogenic differentiation in fibrin-based hydrogels.<sup>141–144</sup>

One of interesting PBM effects, which can be of great practical importance, is its protective ability. It was reported in neurotraumas and neonatal hypoxia-ischemia.<sup>24,145</sup> PBM is mentioned to involve preconditioning mechanisms similar to ischemia, hyperthermia, hypothermia, and

hyperbaric oxygen and is associated with increasing ATP levels, preventing mitochondrial fragmentation and cytochrome c release.<sup>24,25</sup> The PBM effect is most pronounced in weakened cells cultured under nutrient- and growth factor-deficient conditions, which are usually modeled by reducing the serum concentration in the medium.<sup>146–149</sup>

The morphology, physiology, and behavior of cells in scaffolds are determined by the chemical structure of the material, the local topography, architecture, and mechanics of the scaffold.<sup>150</sup> All of these scaffold properties can either enhance or silence the PBM effects.<sup>151</sup> Despite the overall heterogeneity of the PBM parameters reported in papers, some general principles can be revealed. Most of the research is aimed at the stimulation of cell proliferation (to reach a high cell density prior to transplantation of the tissue-engineered construct) or differentiation (to integrate the construct in the host tissue). The transition between proliferation and differentiation is a crucial moment for the cell physiology and can be regulated by PBM.<sup>152,153</sup> Unfortunately, the precise combinations of cell type and particular PBM mode for the specific purpose (e.g., activating proliferation or directing differentiation) are absent now. However, it is known that PBM effects depend on cell type, namely redox systems of the cell.<sup>72,154–156</sup> A recent study has shown the different dynamics and effects of the same PBM mode applied to normal fibroblast or cancer cell lines.<sup>157</sup> The presence of varying metabolic pathways, such as prevailing glycolysis in cancer cell lines, drastically changes the final PBM outcome. Rupel et al. showed that the redox state of the cell can determine the levels of ROS production in cells in response to PBM.<sup>103</sup> Altered mitochondrial state, e.g., caused by exposure to specific mitochondrial complex inhibitors, leads to the various responses. Different inhibitor concentrations either stimulate mitochondrial activity or decrease it even more depending on inhibitor concentration.<sup>71</sup> Moreover, even the amount of mitochondria in cell was connected to observed variabilities in PBM effects.<sup>158</sup> Therefore, the careful choice of cell source, cell type, culturing conditions, and PBM parameters are crucial to predict the cell behavior following PBM.

## 5.1 *Light-Induced Cellular Events Providing the Conditions for Effective Tissue Engineering*

### 5.1.1 *Cellular proliferation*

Cell proliferation is vital for tissue-engineered constructs to achieve viable structures. PBM was shown to maintain the MSCs cell cycle after implementation on a BMP-incorporated scaffold up to the sixth day of cultivation, which resulted in expanded mineral deposition.<sup>159</sup> Similar results were reported in Ref. 160, where ADSCs seeded on an acellular dermal matrix were shown to proliferate and osseointegrate better after the exposure to 633 nm PBM. NIR PBM is also able to influence fibroblast proliferation through the activation of EGF expression.<sup>161</sup> Both red and NIR PBM stimulate metabolic activity and proliferation of gingival MSC encapsulated in a fibrin hydrogel.<sup>101</sup> It seems that PBM activates cell division in sufficiently soft scaffold systems, such as decellularized dermal matrices and hydrogels.<sup>160–162</sup>

### 5.1.2 *Enhanced cellular differentiation*

Numerous studies are dedicated to the stimulation of bone regeneration using PBM, including the exposure of a damaged area without cells transplanted on a scaffold. The aim of PBM, in that case, is to stimulate host cells in bone defects and surrounding tissues. NIR light (730 to 830 nm) increases the efficacy of a titanium scaffold osseointegration in an osteoporosis model, skull bone reparation, and the engraftment of an autologous bone construct.<sup>22,74,163</sup> PBM also helps to organize the surrounding connective tissues in the area of a bone matrix-fibrin construct implantation.<sup>164</sup> Increased levels of transforming growth factor-beta (TGF- $\beta$ ), fibroblast growth factor-2 (FGF-2), osteoprotegerin (OPG), receptor activator of nuclear factor  $\kappa$ B (RANK), osteocalcin (OCN), and BMP-9 in injured bone tissues after PBM were reported.<sup>165,166</sup> In addition, PBM with the wavelength of 780 nm for a ceramic bone graft increased deposition of calcium hydroxyapatite and decrease of the organic components, which is important for healing of fractured bones.<sup>167</sup>

Similar results were observed for cell-loaded scaffolds. When irradiated with red PBM, MSCs differentiate in the osteogenic direction faster in the case of coralline biomatrices, PLGA scaffolds, and an agarose gel.<sup>168–170</sup>

Similarly to the findings discussed above, PBM with the wavelength of 780 nm accelerated the integration of a demineralized bone matrix graft in the periodontal area after alveolar reconstruction surgeries.<sup>73</sup> Some works show that PBM increases the expression of odontogenic markers, such as DSPP, Osterix, RUNX2, BMP-2.<sup>153</sup>

Unlike for osteogenic and odontogenic cells, for neuronal cells, the most preferable 3D system is a hydrogel. It was shown that under the exposure to NIR PBM, embryonic neurons on a hyaluronic acid-based gel acquire adult neuronal morphology.<sup>171</sup> PBM induces the neuronal differentiation and inhibits the glial differentiation of neural stem cells cultivated in a GelMA/PEGDA gel.<sup>172</sup> Red irradiation combined with cross-linked gelatin loaded with ceramic particles is promising for nerve recovery. An increased nerve fiber diameter, myelin sheath thickness, and reduced muscle atrophy around the nerve was noted after PBM.<sup>173</sup>

A few works showed promoted vascularization of HUVECs and human ASCs cocultures in fibrin gels after red PBM.<sup>23</sup> On the other hand, there are some data indicating that PBM has no influence on the angiogenic differentiation of endothelial cells.<sup>174</sup> Both angiogenesis and dentinogenesis of the dentin-pulp complex were shown in a human tooth slice-based *in vitro* model for 810 or 660 nm light with a 1 J/cm<sup>2</sup> intensity.<sup>175</sup>

### 5.1.3 Anti-inflammatory effects

PBM effects on the inflammation processes were broadly studied in different animal models, e.g., burn injury, acute lung injury, and lung fibrosis. The levels of proinflammatory factors, such as TNF- $\alpha$ , NF- $\kappa$ B, IL-6, IL-1 $\beta$ , decreased after red or NIR irradiation.<sup>176–179</sup> It also has been shown that preconditioning with PBM results in reduced levels of proinflammatory cytokines after the induction of inflammation with LPS.<sup>70</sup> The anti-inflammatory activity was revealed also for immune cells. For instance, in the model of lung fibrosis, PBM therapy resulted in reduced infiltration of immune cells into alveolar capillaries.<sup>179</sup> NIR PBM was able to switch M1 (inflammatory) to M2 (anti-inflammatory) polarization of macrophages.<sup>180</sup> Similar effects were shown for PBM *in vitro*: red irradiation induced the transcription of IL-1 $\beta$  and IL-6 mRNA and decreased that of IL-8 in a cultured analog of human skin.<sup>181</sup>

Although the data considering inflammation processes in connection with scaffolds are limited, there is a reason to believe in the effectiveness of PBM. First of all, PBM would be useful to reduce inflammation during transplantation.

### 5.1.4 Biopolymers organization

Since PBM can affect various signaling pathways, biopolymers undergo restructuring, subsequently altering cell behavior. Being both a dynamic structure and a crucial participant of cell signaling pathways, the cytoskeleton is the primary system of biopolymers responding to PBM. Red PBM was shown to induce the arrangement of F-actin molecules.<sup>133</sup> Perhaps, this mechanism underlies the PBM-induced migration of cells within hydrogels.<sup>182</sup> Similar effects were shown in respect to the ECM production. PBM leads not only to the collagen expression and synthesis<sup>161,182</sup> but also to more organized aggregates in comparison to nonirradiated cells.<sup>22</sup> The PBM effects in various conditions are summarized in Table 2.

## 6 Perspectives

The main goal of TE is to create not only tissue-like but also fully functional structures. Although a wide range of 3D cell systems have been presented, they still lack the key features of the target tissue. The next step here is to arrange the complex architecture and cell-specific physiology. Systems such as cellular spheroids or cell sheets offer a list of advantages, including cell interactions, mechanical properties, cell phenotype preservation, etc.<sup>185–188</sup> PBM could be beneficial in that case too: this approach has already been applied to spheroids, cell sheets, and organoids.

**Table 2** Parameters and effects of PBM in scaffolds.

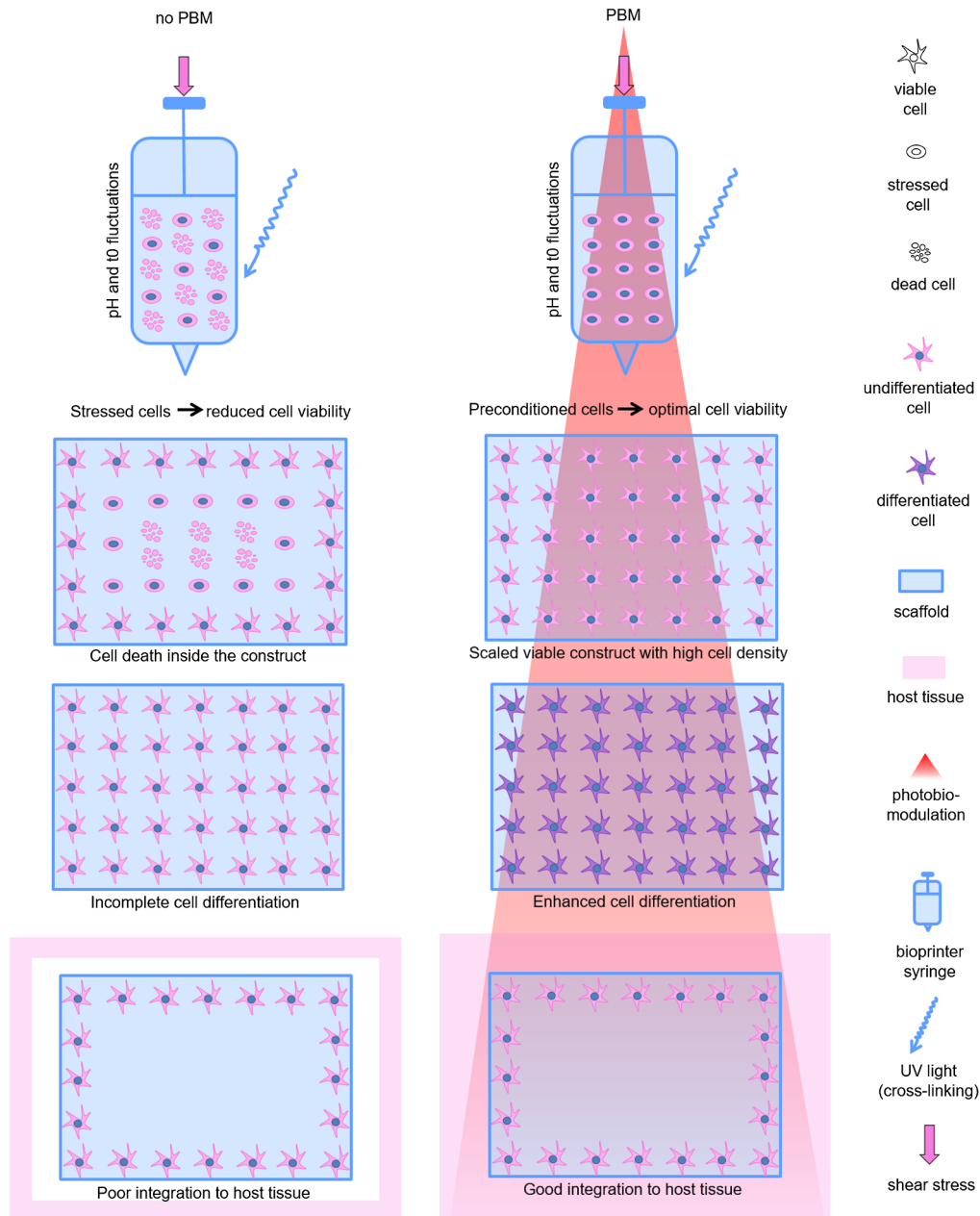
Cell type	Scaffold	Source type	Wavelength (nm)	Energy density (fluence) (J/cm <sup>2</sup> )	Power density (mW/cm <sup>2</sup> )	Cultivation after treatment	Result	Ref.
DPSC	Pluronic® F-127 hydrogel incorporated with BMP4	Laser	660	3 or 5	710	21 days in culture 8 weeks in animals	Increased cell proliferation, acceleration of odonto/osteogenic differentiation	159
Primary gingival fibroblasts	Collagen matrix	LED	780	0.5; 1.5; 3	25	6 days in culture	Enhanced gene expression of hCOL-1 and hEGF and increased cell viability	161
Vero (epithelial cell line)	Porcine serous collagen	LED	630	30	24.1	7 days in culture	Increased ECM deposition and proliferation	162
BM-MSC	Bio-Oss (deproteinized bovine bone)	Laser	810	4	200	3 weeks in animals	New bone formation	74
MSC	Coralline biomatrices	Laser	633	—	0.5 mW	1 to 7, 10, 14, 21, 28 days, culture	Osteogenic differentiation higher ossification levels	168
ADSC	Acellular dermal matrix	Laser	633	1	—	14, 28, 56 days in animals	Increased viability and proliferation, bone regeneration	160
NSC	GeIMA/PEGDA	LED	635	—	10.95	14 days culture	Neuronal differentiation and suppressed glial differentiation	172
Embryonic NSC	NVR-gel (cross-linked hyaluronic acid enriched with laminin, BDNF and IGF-1)	Laser	780	—	20 to 500	24 days in culture	Increased neuronal sprouting	171
DPSC	Mg-based, Zn-doped bioceramic scaffolds	Laser	660	2 or 4, every 3 days	—	28 days culture	Increase of odontogenesis-related markers, newly formed Ca-P tissue was formed	153
HUVEC and ADSC coculture	Fibrin gel	LED	632	24	12	7 days in culture	Promoted vascularization	23

Table 2 (Continued).

Cell type	Scaffold	Source type	Wavelength (nm)	Energy density (fluence) (J/cm <sup>2</sup> )	Power density (mW/cm <sup>2</sup> )	Cultivation after treatment	Result	Ref.
L929 and NIH3T3	Fucoidan/alginate-polyethylene glycol-gellan gum 27 (Fu/AL-PEG@GGH) hydrogel	Laser	635	4	417	1, 2, or 3 days culture	Increased cell migration, cell viability, collagen deposition	182
BM-MSC	Silk scaffolds	Polychromatic plasma arc lamp	590, 633, 666, 712, 812, 1018, 1128, 1356, 1395	—	130	7, 14, or 28 days	Osteogenic differentiation, mineral deposition, F-actin reorganization	133
ADSC	Poly-lactic-co-glycolic acid (PLGA) scaffold	Laser	660	13.3	24.62	16 weeks in animals	New bone formation, osteogenic differentiation	169
MC3T3 (osteoblastic cell line)	Glass-ceramic scaffold (biosilicate)	Laser	830	10	—	7 days in culture	Increased proliferation	183
BM-MSC	Type I collagen scaffold	Laser	810	4; every other day	430	3 weeks in animals	Bone formation	184
DPSC	Agarose gel	Laser	660	3.3; every 6 h	—	7 and 14 days, culture	More effective osteogenic, chondrogenic, or adipogenic differentiation	170

ADSC, adipose-derived stem cells; BM-MSC, bone marrow MSC; DPSC, dental pulp stem cells; MSC, mesenchymal stromal cells; NSC, neural stem cells; HUVEC, human umbilical vein endothelial cells

660-nm PBM induced a complex response in hASC spheroids, including HIF-1 $\alpha$  upregulation, growth factor secretion, cytokeratin expression, angiogenesis, and vascularization in the ischemia model.<sup>75,76</sup> Irradiated DPSC cell sheets expressed high levels of fibronectin and had epithelium-like cell phenotypes.<sup>189</sup> These sheets also exhibited increased osteogenic differentiation.<sup>190</sup> Moreover, the PBM ability to induce differentiation allowed triggering a specific direction of embryonic stem cell differentiation, which resulted in the successful formation of otic organoids.<sup>191</sup> Although there is a restricted amount of such works, they are important in the context of the TE. Taking into account the beneficial effects often observed for cells in various 3D scaffolds reviewed here, the future research should be focused on the PBM utilization for the cell survival, proliferation, and differentiation in 3D scaffolds. As PBM devices are highly



**Fig. 4** The possibilities of PBM to stimulate various aspects of cell physiology in 3D tissue engineered constructs (scaffolds or hydrogels) during the bioprinting, cultivation, differentiation, and transplantation.

available, easy-to-use, tunable, and have been already certified for the clinical practice, the new combinations of biofabrication approaches with PBM are to be expected.

However, it is still hard to predict the effects of PBM, especially in 3D systems, due to the different cell type and redox status, 3D scaffold composition, and optical properties. The PBM mechanisms involving light scattering and absorption should be clarified. However, despite all the variables, the current review suggests the high PBM potential in the field of TE, in particular for scaffolds and 3D bioprinting. Such techniques are favorable to resemble native tissue structure, but they face a few crucial limitations. Bioprinted cells suffer from shear stress, UV light during crosslinking, and temperature changes (Fig. 4). PBM sources are technically easy to introduce to bioprinters to deliver light to weakened cells in optically transparent hydrogels or scaffolds. Such modification of bioprinting approaches could increase the survivability of the scalable tissue equivalent.

PBM has currently begun being applied in numerous fields of TE, and some researchers even propose PBM as a novel fourth component of the TE triad among stem cells, scaffolds, and growth factors.<sup>192</sup>

## 7 Conclusion

Taken all together, scaffold-based tissue-engineered constructs and PBM complement each other. PBM stimulating wavelengths match with the optical transparency of a scaffold, and decreased cell viability after seeding in the scaffold is an object for the PBM preconditioning effect. PBM in the red and NIR ranges was shown to be effective for the stimulation of cell survival, proliferation, and differentiation in the conditions of various 3D systems. The careful selection of the PBM wavelength and intensity, coupled with the latest TE approaches, will lead to taking one step closer to creating functional and scaled tissue-like constructs.

## Disclosure

The authors declare no conflict of interest.

## Acknowledgments

Research at Sechenov University was funded by the Ministry of Science and Higher Education of the Russian Federation under the Grant Agreement No. 075-15-2021-596. The authors thank Svetlana Kotova for the proofreading of the manuscript. The study was performed using the unique scientific facility Transgenebank.

## References

1. J. J. Anders, R. J. Lanzafame, and P. R. Arany, "Low-level light/laser therapy versus photobiomodulation therapy," *Photomed. Laser Surg.* **33**(4), 183–184 (2015).
2. M. R. Hamblin, Y.-Y. Huang, and V. Heiskanen, "Non-mammalian hosts and photobiomodulation: do all life-forms respond to light?" *Photochem. Photobiol.* **95**(1), 126–139 (2019).
3. A. K. Burditt, "Irradiation," in *Quarantine Treatments for Pests of Food Plants*, pp. 101–117, CRC Press (1994).
4. R. Fekrazad et al., "Effect of photobiomodulation on mesenchymal stem cells," *Photomed. Laser Surg.* **34**(11), 533–542 (2016).
5. R. Yin et al., "Light based anti-infectives: ultraviolet C irradiation, photodynamic therapy, blue light, and beyond," *Curr. Opin. Pharmacol.* **13**(5), 731–762 (2013).
6. A. Mester and A. Mester, "The history of photobiomodulation: Endre Mester (1903–1984)," *Photomed. Laser Surg.* **35**, 393–394 (2017).
7. E. Mester et al., "Effect of laser rays on wound healing," *Am. J. Surg.* **122**(4), 532–535 (1971).

8. A. Xiang et al., "Laser photobiomodulation for cartilage defect in animal models of knee osteoarthritis: a systematic review and meta-analysis," *Lasers Med. Sci.* **35**(4), 789–796 (2019).
9. M. P. O. Rosso et al., "Photobiomodulation therapy (PBMT) applied in bone reconstructive surgery using bovine bone grafts: a systematic review," *Materials-Basel, Switzerland* **12**(24), 4051 (2019).
10. F. Salehpour et al., "Brain photobiomodulation therapy: a narrative review," *Mol. Neurobiol.* **55**, 6601–6636 (2018).
11. M. V. P. de Sousa et al., "Pain management using photobiomodulation: mechanisms, location, and repeatability quantified by pain threshold and neural biomarkers in mice," *J. Biophotonics* **11**(7), e201700370 (2018).
12. T. Walski et al., "The effect of red-to-near-infrared (R/NIR) irradiation on inflammatory processes," *Int. J. Radiat. Biol.* **95**, 1326–1336 (2019).
13. A. Lamaro-Cardoso et al., "Photobiomodulation associated to cellular therapy improve wound healing of experimental full thickness burn wounds in rats," *J. Photochem. Photobiol. B Biol.* **194**, 174–182 (2019).
14. R. Brignardello-Petersen, "Uncertainty about usefulness of low-level laser therapy for improving implant outcomes," *J. Am. Dent. Assoc.* **149**(3), e55 (2018).
15. S. Wang et al., "Shedding light on the FDA's 510(k) approvals process: low-level laser therapy devices used in the treatment of androgenetic alopecia," *J. Dermatol. Treat.* **30**(5), 489–491 (2019).
16. T. C. Wikramanayake et al., "Effects of the Lexington LaserComb on hair regrowth in the C3H/HeJ mouse model of alopecia areata," *Lasers Med. Sci.* **27**(2), 431–436 (2012).
17. T. I. Karu, *Ten Lectures on Basic Science of Laser Phototherapy*, p. 414, Prima Books (2007).
18. L. F. de Freitas and M. R. Hamblin, "Proposed mechanisms of photobiomodulation or low-level light therapy," *IEEE J. Sel. Top. Quantum Electron.* **22**(3), 348–364 (2016).
19. K. Yin et al., "Low-level laser effect on proliferation, migration, and antiapoptosis of mesenchymal stem cells," *Stem Cells Dev.* **26**(10), 762–775 (2017).
20. A. G. Yodh and D. A. Boas, "Functional imaging with diffusing light," in *Biomedical Photonics Handbook*, pp. 311–356, CRC Press (2014).
21. V. I. Yusupov et al., "The regulatory effect of low-intensity radiation in the near-infrared region on the early development of zebrafish (*Danio rerio*)," *Biophysics* **63**(1), 109–115 (2018).
22. L. M. R. de Vasconcellos et al., "Erratum to: titanium scaffold osteogenesis in healthy and osteoporotic rats is improved by the use of low-level laser therapy (GaAlAs)," *Lasers Med. Sci.* **31**, 899–905 (2016); *Lasers Med. Sci.* **32**(3), 733 (2017).
23. R. Winter et al., "Photobiomodulation (PBM) promotes angiogenesis *in-vitro* and in chick embryo chorioallantoic membrane model," *Sci. Rep.* **8**, 17080 (2018).
24. L. Yang et al., "Photobiomodulation preconditioning prevents cognitive impairment in a neonatal rat model of hypoxia-ischemia," *J. Biophotonics* **12**(6), e201800359 (2019).
25. T. Agrawal et al., "Pre-conditioning with low-level laser (light) therapy: light before the storm," *Dose-Response* **12**(4), 619–649 (2014).
26. M. W. Tibbitt and K. S. Anseth, "Hydrogels as extracellular matrix mimics for 3D cell culture," *Biotechnol. Bioeng.* **103**, 655–663 (2009).
27. B. M. Baker and C. S. Chen, "Deconstructing the third dimension-how 3D culture micro-environments alter cellular cues," *J. Cell Sci.* **125**, 3015–3024 (2012).
28. K. Duval et al., "Modeling physiological events in 2D vs. 3D cell culture," *Physiology* **32**(4), 266–277 (2017).
29. J. C. Fontoura et al., "Comparison of 2D and 3D cell culture models for cell growth, gene expression and drug resistance," *Mater. Sci. Eng. C* **107**, 110264 (2020).
30. R. C. Dutta and A. K. Dutta, "Cell-interactive 3D-scaffold; advances and applications," *Biotechnol. Adv.* **27**(4), 334–339 (2009).
31. W. Bensaïd et al., "A biodegradable fibrin scaffold for mesenchymal stem cell transplantation," *Biomaterials* **24**(14), 2497–2502 (2003).



32. H. T. Kang et al., "Effect of stem cell treatment on acute liver failure model using scaffold," *Dig. Dis. Sci.* **64**(3), 781–791 (2019).
33. M. Asmani et al., "Fibrotic microtissue array to predict anti-fibrosis drug efficacy," *Nat. Commun.* **9**, 2066 (2018).
34. P. Timashev et al., "Novel biodegradable star-shaped polylactide scaffolds for bone regeneration fabricated by two-photon polymerization," *Nanomedicine* **11**(9), 1041–1053 (2016).
35. A. Shpichka et al., "Skin tissue regeneration for burn injury," *Stem Cell Res. Ther.* **10**, 94 (2019).
36. J. Malda, T. J. Klein, and Z. Upton, "The roles of hypoxia in the *in vitro* engineering of tissues," *Tissue Eng.* **13**(9), 2153–2162 (2007).
37. J. Riesle et al., "Oxygen gradients in tissue-engineered Pegt/Pbt cartilaginous constructs: measurement and modeling," *Biotechnol. Bioeng.* **86**(1), 9–18 (2004).
38. L. Figueiredo et al., "Assessing glucose and oxygen diffusion in hydrogels for the rational design of 3D stem cell scaffolds in regenerative medicine," *J. Tissue Eng. Regen. Med.* **12**(5), 1238–1246 (2018).
39. M. Vidotto, D. Dini, and E. De Momi, "Effective diffusion and tortuosity in brain white matter," in *Proc. Annu. Int. Conf. IEEE Eng. in Med. and Biol. Soc., EMBS*, Institute of Electrical and Electronics Engineers Inc., pp. 4901–4904 (2018).
40. A. M. Römgens et al., "Diffusion profile of macromolecules within and between human skin layers for (trans)dermal drug delivery," *J. Mech. Behav. Biomed. Mater.* **50**, 215–222 (2015).
41. R. J. McMurtrey, "Analytic models of oxygen and nutrient diffusion, metabolism dynamics, and architecture optimization in three-dimensional tissue constructs with applications and insights in cerebral organoids," *Tissue Eng. Part C Methods* **22**(3), 221–249 (2016).
42. J. R. Dorvee, A. L. Boskey, and L. A. Estroff, "Rediscovering hydrogel-based double-diffusion systems for studying biomineralization," *CrystEngComm* **14**(18), 5681–700 (2012).
43. S. Ramanujan et al., "Diffusion and convection in collagen gels: implications for transport in the tumor interstitium," *Biophys. J.* **83**(3), 1650–1660 (2002).
44. F. Sauer et al., "Collagen networks determine viscoelastic properties of connective tissues yet do not hinder diffusion of the aqueous solvent," *Soft Matter* **15**(14), 3055–3064 (2019).
45. I. Westphal et al., "Oxygen mapping: probing a novel seeding strategy for bone tissue engineering," *Biotechnol. Bioeng.* **114**(4), 894–902 (2017).
46. S. Bahsoun et al., "The role of dissolved oxygen levels on human mesenchymal stem cell culture success, regulatory compliance, and therapeutic potential," *Stem Cells Dev.* **27**, 1303–1321 (2018).
47. C. Holzwarth et al., "Low physiologic oxygen tensions reduce proliferation and differentiation of human multipotent mesenchymal stromal cells," *BMC Cell Biol.* **11**, 11 (2010).
48. J. R. Choi et al., "Impact of low oxygen tension on stemness, proliferation and differentiation potential of human adipose-derived stem cells," *Biochem. Biophys. Res. Commun.* **448**(2), 218–224 (2014).
49. A. G. Ardakani et al., "Quantifying the correlation between spatially defined oxygen gradients and cell fate in an engineered three-dimensional culture model," *J. R. Soc. Interface* **11**(98), 20140501 (2014).
50. D. R. Grimes et al., "Estimating oxygen distribution from vasculature in three-dimensional tumour tissue," *J. R. Soc. Interface* **13**(116), 20160070 (2016).
51. E. Volkmer et al., "Hypoxia in static and dynamic 3D culture systems for tissue engineering of bone," *Tissue Eng. - Part A* **14**(8), 1331–1340 (2008).
52. M. J. Farrell et al., "Functional consequences of glucose and oxygen deprivation on engineered mesenchymal stem cell-based cartilage constructs," *Osteoarthr. Cartil.* **23**(1), 134–142 (2015).
53. K. E. Schlageter et al., "Microvessel organization and structure in experimental brain tumors: microvessel populations with distinctive structural and functional properties," *Microvasc. Res.* **58**(3), 312–328 (1999).

54. D. Wendt et al., "Uniform tissues engineered by seeding and culturing cells in 3D scaffolds under perfusion at defined oxygen tensions," *Biorheology* **43**(3–4), 481–488 (2006).
55. M. C. Lewis et al., "Heterogeneous proliferation within engineered cartilaginous tissue: the role of oxygen tension," *Biotechnol. Bioeng.* **91**(5), 607–615 (2005).
56. M. Radisic et al., "Mathematical model of oxygen distribution in engineered cardiac tissue with parallel channel array perfused with culture medium containing oxygen carriers," *Am. J. Physiol. Circ. Physiol.* **288**(3), H1278–H1289 (2005).
57. A. K. Miri et al., "Permeability mapping of gelatin methacryloyl hydrogels," *Acta Biomater.* **77**, 38–47 (2018).
58. H. T. Whelan et al., "Effect of NASA light-emitting diode irradiation on wound healing," *J. Clin. Laser Med. Surg.* **19**(6), 305–314 (2001).
59. L. Yue and M. S. Humayun, "Monte Carlo analysis of the enhanced transcranial penetration using distributed near-infrared emitter array," *J. Biomed. Opt.* **20**(8), 088001 (2015).
60. T. A. Henderson and L. D. Morries, "Near-infrared photonic energy penetration: can infrared phototherapy effectively reach the human brain?" *Neuropsychiatr. Dis. Treat.* **11**, 2191–208 (2015).
61. D. Hao et al., "Hypoxic preconditioning enhances survival and proangiogenic capacity of human first trimester chorionic Villus-derived mesenchymal stem cells for fetal tissue engineering," *Stem Cells Int.* **2019**, 9695239 (2019).
62. M. Zhang et al., "Cardiomyocyte grafting for cardiac repair: graft cell death and anti-death strategies," *J. Mol. Cell Cardiol.* **33**(5), 907–921 (2001).
63. K. Moeinabadi-Bidgoli et al., "Translational insights into stem cell preconditioning: from molecular mechanisms to preclinical applications," *Biomed. Pharmacother.* **142**, 112026 (2021).
64. J. H. Lee, Y. M. Yoon, and S. H. Lee, "Hypoxic preconditioning promotes the bioactivities of mesenchymal stem cells via the HIF-1 $\alpha$ -GRP78-Akt axis," *Int. J. Mol. Sci.* **18**(6), 1320 (2017).
65. J. Zhang et al., "Hydrogen peroxide preconditioning enhances the therapeutic efficacy of Wharton's jelly mesenchymal stem cells after myocardial infarction," *Chin. Med. J.* **125**(19), 3472–3478 (2012).
66. L. Teng, E. Bennett, and C. Cai, "Preconditioning c-kit-positive human cardiac stem cells with a nitric oxide donor enhances cell survival through activation of survival signaling pathways," *J. Biol. Chem.* **291**(18), 9733–9747 (2016).
67. J. H. Cui et al., "Preconditioning of mesenchymal stem cells with low-intensity ultrasound for cartilage formation *in vivo*," *Tissue Eng.* **13**(2), 351–360 (2007).
68. H. A. Mena et al., "Acidic preconditioning of endothelial colony-forming cells (ECFC) promote vasculogenesis under proinflammatory and high glucose conditions *in vitro* and *in vivo*," *Stem Cell Res. Ther.* **9**(1), 1–13 (2018).
69. J. M. C. de la Barca et al., "Retinal metabolic events in preconditioning light stress as revealed by wide-spectrum targeted metabolomics," *Metabolomics* **13**(3), 22 (2017).
70. A. Bartos et al., "Pre-conditioning with near infrared photobiomodulation reduces inflammatory cytokines and markers of oxidative stress in cochlear hair cells," *J. Biophotonics* **9**(11–12), 1125–1135 (2016).
71. P. Y. Bikmulina et al., "Photobiomodulation enhances mitochondrial respiration in an *in vitro* rotenone model of Parkinson's disease," *Opt. Eng.* **59**(6), 061620 (2020).
72. M. R. Hamblin, "Mechanisms and mitochondrial redox signaling in photobiomodulation," *Photochem. Photobiol.* **94**(2), 199–212 (2018).
73. K. A. Kim et al., "Effect of low-level laser therapy on orthodontic tooth movement into bone-grafted alveolar defects," *Am. J. Orthod. Dentofac Orthop.* **148**(4), 608–617 (2015).
74. R. Fekrazad et al., "The effects of combined low level laser therapy and mesenchymal stem cells on bone regeneration in rabbit calvarial defects," *J. Photochem. Photobiol. B Biol.* **151**, 180–185 (2015).
75. I.-S. Park, P.-S. Chung, and J. C. Ahn, "Angiogenic synergistic effect of adipose-derived stromal cell spheroids with low-level light therapy in a model of acute skin flap ischemia," *Cells Tissues Organs* **202**(5–6), 307–318 (2016).

76. I. S. Park, P. S. Chung, and J. C. Ahn, “Enhanced angiogenic effect of adipose-derived stromal cell spheroid with low-level light therapy in hind limb ischemia mice,” *Biomaterials* **35**(34), 9280–9289 (2014).
77. A. Teuschl et al., “Phototherapy with LED light modulates healing processes in an *in vitro* scratch-wound model using 3 different cell types,” *Dermatol. Surg.* **41**(2), 261–268 (2015).
78. T. I. Karu and S. F. Kolyakov, “Exact action spectra for cellular responses relevant to phototherapy,” *Photomed. Laser Surg.* **23**(4), 355–361 (2005).
79. S. I. Parenti et al., “Effect of low-level laser irradiation on osteoblast-like cells cultured on porous hydroxyapatite scaffolds,” *Ann. Ist. Super Sanita* **49**(3), 255–260 (2013).
80. A. P. Sommer et al., “Biostimulatory windows in low-intensity laser activation: lasers, scanners, and NASA’s light-emitting diode array system,” *J. Clin. Laser Med. Surg.* **19**(1), 29–33 (2001).
81. N. V. Andreeva et al., “Cytotoxic effect of low-intensity infrared laser irradiation on human melanoma cells,” *Mol. Biol.* **52**(6), 878–890 (2018).
82. N. V. Andreeva et al., “The effect of infrared laser irradiation on the growth of human melanoma cells in culture,” *Biophysics* **61**(6), 979–984 (2016).
83. H. Chung et al., “The nuts and bolts of low-level laser (light) therapy,” *Ann. Biomed. Eng.* **40**(2), 516–533 (2012).
84. T. I. Karu, “Molecular mechanisms of the therapeutic effect of low-intensity laser radiation,” *Lasers Life Sci.* **2**(1), 53–74 (1988).
85. V. Heiskanen and M. R. Hamblin, “Photobiomodulation: lasers vs. light emitting diodes?” *Photochem. Photobiol. Sci.* **17**(8), 1003–1017 (2018).
86. M. R. Hamblin, “How to write a good photobiomodulation article,” *Photobiomod. Photomed. Laser Surg.* **37**(6), 325–326 (2019).
87. D. E. Hudson et al., “Penetration of laser light at 808 and 980 nm in bovine tissue samples,” *Photomed. Laser Surg.* **31**(4), 163 (2013).
88. C. E. Tedford et al., “Quantitative analysis of transcranial and intraparenchymal light penetration in human cadaver brain tissue,” *Lasers Surg. Med.* **47**(4), 312–322 (2015).
89. N. Kampa et al., “Penetration depth study of 830 nm low-intensity laser therapy on living dog tissue,” *Vet. World* **13**(7), 1417–1422 (2020).
90. A. P. P. Sviridov et al., “Optical fields in porous polylactide matrices,” *Quantum Electron.* **50**(1), 81–86 (2020).
91. A. J. Welch and M. J. C. Van Gemert, “Optical-thermal response of laser-irradiated tissue,” in *Optical-Thermal Response of Laser-Irradiated Tissue*, pp. 1–958, Springer Netherlands (2011).
92. V. V. Tuchin, *Tissue Optics: Light Scattering Methods and Instruments for Medical Diagnosis*, 3rd ed., SPIE Press, Bellingham, Washington (2015).
93. V. V. Tuchin, “Tissue optics and photonics: light-tissue interaction,” *J. Biomed. Photonics Eng.* **1**(1), 98–134 (2015).
94. C. Ash et al., “Effect of wavelength and beam width on penetration in light-tissue interaction using computational methods,” *Lasers Med. Sci.* **32**(8), 1909–1918 (2017).
95. V. V. Tuchin, *Handbook of Optical Biomedical Diagnostics, Volume 2: Methods*, Vol. 2, p. 642, SPIE (2016).
96. M. Hiraoka et al., “A Monte Carlo investigation of optical pathlength in inhomogeneous tissue and its application to near-infrared spectroscopy,” *Phys. Med. Biol.* **38**(12), 1859 (1993).
97. V. Yusupov et al., “Optical and thermal fields induced in the bone marrow by external laser irradiation,” *Lasers Med. Sci.* **37**(2), 1245–1253 (2022).
98. O. V. Vorob’yeva et al., “Effects of He–Ne laser on *Daphnia magna* Straus manifested in subsequent generations,” *Laser Phys. Lett.* **12**(11), 115601 (2015).
99. R. Kohli, P. K. Gupta, and A. Dube, “Helium-neon laser preirradiation induces protection against UVC radiation in wild-type *E. coli* strain K12AB1157,” *Radiat. Res.* **153**(2), 181–185 (2000).
100. I. Moreno and C.-C. Sun, “Modeling the radiation pattern of LEDs,” *Opt. Express* **16**(3), 1808 (2008).

101. P. Y. Bikmulina et al., “Beyond 2D: effects of photobiomodulation in 3D tissue-like systems,” *J. Biomed. Opt.* **25**(4), 048001 (2020).
102. B. P. Chan et al., “Photochemical cross-linking for collagen-based scaffolds: a study on optical properties, mechanical properties, stability, and hematocompatibility,” *Tissue Eng.* **13**(1), 73–85 (2007).
103. K. Rupel et al., “Photobiomodulation at multiple wavelengths differentially modulates oxidative stress *in vitro* and *in vivo*,” *Oxid. Med. Cell Longev.* **2018**, 1 (2018).
104. A. D. Camacho, D. Montoya Guzmán, and S. A. Velásquez Cujar, “Effective wavelength range in photobiomodulation for tooth movement acceleration in orthodontics: a systematic review,” *Photobiomod. Photomed. Laser Surg.* **38**(10), 581–590 (2020).
105. S. A. Guaraldo et al., “The effect of low-level laser therapy on oxidative stress and functional fitness in aged rats subjected to swimming: an aerobic exercise,” *Lasers Med. Sci.* **31**(5), 833–840 (2016).
106. S. A. Dos Santos et al., “Effects of photobiomodulation therapy on oxidative stress in muscle injury animal models: a systematic review,” *Oxid. Med. Cell Longev.* **2017**, 5273403 (2017).
107. M. R. Hamblin and M. R. Hamblin, “Mechanisms and applications of the anti-inflammatory effects of photobiomodulation,” *AIMS Biophys.* **4**(3), 337–361 (2017).
108. T. I. Karu, “Mitochondrial signaling in mammalian cells activated by red and near-IR radiation,” *Photochem. Photobiol.* **84**(5), 1091–1099 (2008).
109. A. N. Osipov, G. G. Borisenko, and Y. A. Vladimirov, “Biological activity of hemoprotein nitrosyl complexes,” *Biochemistry* **72**(13), 1491–1504 (2007).
110. M. G. Mason, P. Nicholls, and C. E. Cooper, “Re-evaluation of the near infrared spectra of mitochondrial cytochrome c oxidase: implications for non invasive *in vivo* monitoring of tissues,” *Biochim. Biophys. Acta - Bioenerg.* **1837**(11), 1882–1891 (2014).
111. T. I. Karu, “Multiple roles of cytochrome c oxidase in mammalian cells under action of red and IR-A radiation,” *IUBMB Life* **62**(8), 607–610 (2010).
112. D. J. Stuehr, “Mammalian nitric oxide synthases,” *Biochim. Biophys. Acta – Bioenerg.* **1411**(2–3), 217–230 (1999).
113. D. A. Wink et al., “Mechanisms of the antioxidant effects of nitric oxide,” *Antioxid. Redox. Signal* **3**(2), 203–213 (2001).
114. G. C. Brown, “Regulation of mitochondrial respiration by nitric oxide inhibition of cytochrome c oxidase,” *Biochim. Biophys. Acta – Bioenerg.* **1504**(1), 46–57 (2001).
115. M. W. J. Cleeter et al., “Reversible inhibition of cytochrome c oxidase, the terminal enzyme of the mitochondrial respiratory chain, by nitric oxide. Implications for neurodegenerative diseases,” *FEBS Lett.* **345**(1), 50–54 (1994).
116. E. A. Buravlev et al., “Effects of laser and LED radiation on mitochondrial respiration in experimental endotoxic shock,” *Lasers Med. Sci.* **28**(3), 785–790 (2013).
117. Y. Wang et al., “Red (660 nm) or near-infrared (810 nm) photobiomodulation stimulates, while blue (415 nm), green (540 nm) light inhibits proliferation in human adipose-derived stem cells,” *Sci. Rep.* **7**(1), 7781 (2017).
118. S. George, M. R. Hamblin, and H. Abrahamse, “Effect of red light and near infrared laser on the generation of reactive oxygen species in primary dermal fibroblasts,” *J. Photochem. Photobiol. B Biol.* **188**, 60–68 (2018).
119. R. Lubart et al., “Low-energy laser irradiation promotes cellular redox activity,” *Photomed. Laser Surg.* **23**, 3–9 (2005).
120. J. Zhang et al., “ROS and ROS-mediated cellular signaling,” *Oxid. Med. Cell Longev.* **2016**, 4350965 (2016).
121. H. Friedmann et al., “A possible explanation of laser-induced stimulation and damage of cell cultures,” *J. Photochem. Photobiol. B: Biol.* **11**, 87–91 (1991).
122. I. Golovynska et al., “Red and near-infrared light evokes Ca<sup>2+</sup> influx, endoplasmic reticulum release and membrane depolarization in neurons and cancer cells,” *J. Photochem. Photobiol. B Biol.* **214**, 112088 (2021).
123. L. Munaron, S. Antoniotti, and D. Lovisolo, “Intracellular calcium signals and control of cell proliferation: how many mechanisms?” *J. Cell Mol. Med.* **8**(2), 161–168 (2004).

124. Y. Zhang et al., "cDNA microarray analysis of gene expression profiles in human fibroblast cells irradiated with red light," *J. Invest. Dermatol.* **120**(5), 776–780 (2003).
125. T. D. Gilmore, "Introduction to NF- $\kappa$ B: players, pathways, perspectives," *Oncogene* **25**(51), 6680–6684 (2006).
126. A. de Farias Gabriel et al., "Photobiomodulation therapy modulates epigenetic events and NF- $\kappa$ B expression in oral epithelial wound healing," *Lasers Med. Sci.* **34**(7), 1465–1472 (2019).
127. D. Trachootham et al., "Redox regulation of cell survival," *Antioxid. Redox. Signal* **10**(8), 1343–1374 (2010).
128. N. Li and M. Karin, "Is NF- $\kappa$ B the sensor of oxidative stress?" *FASEB J.* **13**(10), 1137–1143 (1999).
129. A. Borzabadi-Farahani, "Effect of low-level laser irradiation on proliferation of human dental mesenchymal stem cells; a systemic review," *J. Photochem. Photobiol. B Biol.* **162**, 577–582 (2016).
130. M. Giannelli et al., "Photoactivation of bone marrow mesenchymal stromal cells with diode laser: effects and mechanisms of action," *J. Cell Physiol.* **228**(1), 172–181 (2013).
131. X. Gao et al., "Single cell analysis of PKC activation during proliferation and apoptosis induced by laser irradiation," *J. Cell Physiol.* **206**(2), 441–448 (2006).
132. R. Fekrazad et al., "Photobiomodulation with single and combination laser wavelengths on bone marrow mesenchymal stem cells: proliferation and differentiation to bone or cartilage," *Lasers Med. Sci.* **34**(1), 115–126 (2019).
133. A. S. Çakmak et al., "Photostimulation of osteogenic differentiation on silk scaffolds by plasma arc light source," *Lasers Med. Sci.* **33**(4), 785–794 (2018).
134. D. G. Duda, D. Fukumura, and R. K. Jain, "Role of eNOS in neovascularization: NO for endothelial progenitor cells," *Trends Mol. Med.* **10**(4), 143–145 (2004).
135. L. V. Faria et al., "Photobiomodulation can prevent apoptosis in cells from mouse periodontal ligament," *Lasers Med. Sci.* **35**(8), 1841–1848 (2020).
136. A. Janzadeh, "Photobiomodulation therapy reduces apoptotic factors and increases glutathione levels in a neuropathic pain model," *Lasers Med. Sci.* **31**(9), 1863–1869 (2016).
137. L. C. Gomes, G. Di Benedetto, and L. Scorrano, "During autophagy mitochondria elongate, are spared from degradation and sustain cell viability," *Nat. Cell Biol.* **13**(5), 589–598 (2011).
138. K. Labbé, A. Murley, and J. Nunnari, "Determinants and functions of mitochondrial behavior," *Annu. Rev. Cell Dev. Biol.* **30**(1), 357–391 (2014).
139. J. C. Tatmatsu-Rocha et al., "Mitochondrial dynamics (fission and fusion) and collagen production in a rat model of diabetic wound healing treated by photobiomodulation: comparison of 904 nm laser and 850 nm light-emitting diode (LED)," *J. Photochem. Photobiol. B Biol.* **187**, 41–47 (2018).
140. F. Zare et al., "Photobiomodulation with 630 plus 810 nm wavelengths induce more in vitro cell viability of human adipose stem cells than human bone marrow-derived stem cells," *J. Photochem. Photobiol. B Biol.* **1**, 201 (2019).
141. A. I. Shpichka et al., "Digging deeper: Structural background of PEGylated fibrin gels in cell migration and lumenogenesis," *RSC Adv.* **10**(8), 4190–4200 (2020).
142. A. I. Shpichka et al., "Evaluation of the vasculogenic potential of hydrogels based on modified fibrin," *Cell Tissue Biol.* **11**(1), 81–87 (2017).
143. T. Ruckh et al., "Mineralization content alters osteogenic responses of bone marrow stromal cells on hydroxyapatite/polycaprolactone composite nanofiber scaffolds," *J. Funct. Biomater.* **3**(4), 776–798 (2012).
144. V. A. Revkova et al., "Chitosan-g-oligo(L,L-lactide) copolymer hydrogel potential for neural stem cell differentiation," *Tissue Eng. - Part A* **26**(17–18), 953–963 (2020).
145. V. Ganeshan et al., "Pre-conditioning with remote photobiomodulation modulates the brain transcriptome and protects against MPTP insult in mice," *Neuroscience* **400**, 85–97 (2019).
146. A. P. Fernandes et al., "Effects of low-level laser therapy on stem cells from human exfoliated deciduous teeth," *J. Appl. Oral Sci.* **24**(4), 332–337 (2016).

147. C. Moura-Netto et al., "Low-intensity laser phototherapy enhances the proliferation of dental pulp stem cells under nutritional deficiency," *Braz. Oral Res.* **30**(1), S1806–83242016000100265 (2016).
148. I. V. Vakhruhev et al., "Effect of low-level laser irradiation on proliferative activity of Wharton's jelly mesenchymal stromal cells," *Bull. Exp. Biol. Med.* **167**(1), 136–139 (2019).
149. R. K. Chailakhyan et al., "Activation of bone marrow multipotent stromal cells by laser and EHF radiation and their combined impacts," *Sovrem. Tehnol. v. Med.* **9**(1), 28 (2017).
150. P. Bikmulina et al., "3D or not 3D: a guide to assess cell viability in 3D cell systems," *Soft Matter* **18**(11), 2222–2233 (2022).
151. A. C. M. Renno et al., "Effect of 830-nm laser phototherapy on olfactory neuronal ensheathing cells grown in vitro on novel bioscaffolds," *J. Appl. Biomater. Funct. Mater.* **13**(3), e234–e240 (2015).
152. R. Strehl et al., "Proliferating cells versus differentiated cells in tissue engineering," *Tissue Eng.* **8**(1), 37–42 (2002).
153. A. Theocharidou et al., "Odontogenic differentiation and biomineralization potential of dental pulp stem cells inside Mg-based bioceramic scaffolds under low-level laser treatment," *Lasers Med. Sci.* **32**(1), 201–210 (2017).
154. B. Ahrabi et al., "The effect of photobiomodulation therapy on the differentiation, proliferation, and migration of the mesenchymal stem cell: a review," *J. Lasers Med. Sci.* **10**, S96–S103 (2019).
155. K. W. Engel, I. Khan, and P. R. Arany, "Cell lineage responses to photobiomodulation therapy," *J. Biophotonics* **9**(11–12), 1148–1156 (2016).
156. T. Karu, "Photochemical effects upon the cornea, skin and other tissues," *Photobiol. Low-Power Laser Eff.* **56**(5), 1–20 (1986).
157. C. M. G. de Faria et al., "Effects of photobiomodulation on the redox state of healthy and cancer cells," *Biomed. Opt. Express* **12**(7), 3902–3916 (2021).
158. H. J. Serrage et al., "Differential responses of myoblasts and myotubes to photobiomodulation are associated with mitochondrial number," *J. Biophotonics* **12**(6), e201800411 (2019).
159. I. M. A. Diniz et al., "Photobiomodulation of mesenchymal stem cells encapsulated in an injectable rhBMP4-loaded hydrogel directs hard tissue bioengineering," *J. Cell Physiol.* **233**(6), 4907–4918 (2018).
160. K. Choi et al., "Low-level laser therapy promotes the osteogenic potential of adipose-derived mesenchymal stem cells seeded on an acellular dermal matrix," *J. Biomed. Mater. Res. – Part B Appl. Biomater.* **101B**(6), 919–928 (2013).
161. F. G. Basso et al., "Low-level laser therapy in 3D cell culture model using gingival fibroblasts," *Lasers Med. Sci.* **31**(5), 973–978 (2016).
162. A. C. B. Oliveira et al., "Red light accelerates the formation of a human dermal equivalent," *J. Biomater. Appl.* **32**(9), 1265–1275 (2018).
163. J. B. de Oliveira Gonçalves et al., "Effects of low-level laser therapy on autogenous bone graft stabilized with a new heterologous fibrin sealant," *J. Photochem. Photobiol. B Biol.* **162**, 663–668 (2016).
164. M. P. de Oliveria Rosso et al., "Photobiomodulation therapy associated with heterologous fibrin biopolymer and bovine bone matrix helps to reconstruct long bones," *Biomolecules* **10**(3), 383 (2020).
165. L. S. S. de Oliveira et al., "Low-level laser therapy (780 nm) combined with collagen sponge scaffold promotes repair of rat cranial critical-size defects and increases TGF- $\beta$ , FGF-2, OPG/RANK and osteocalcin expression," *Int. J. Exp. Pathol.* **98**(2), 75–85 (2017).
166. K. N. Z. Pinto et al., "Effects of biosilicate<sup>®</sup> scaffolds and low-level laser therapy on the process of bone healing," *Photomed. Laser Surg.* **31**(6), 252–260 (2013).
167. A. L. B. Pinheiro et al., "The efficacy of the use of IR laser phototherapy associated to biphasic ceramic graft and guided bone regeneration on surgical fractures treated with wire osteosynthesis: a comparative laser fluorescence and Raman spectral study on rabbits," *Lasers Med. Sci.* **28**(3), 815–822 (2013).

168. L. Abramovitch-Gottlieb et al., "Low level laser irradiation stimulates osteogenic phenotype of mesenchymal stem cells seeded on a three-dimensional biomatrix," *Lasers Med. Sci.* **20**(3–4), 138–146 (2005).
169. Y. H. Wang et al., "Low power laser irradiation and human adipose-derived stem cell treatments promote bone regeneration in critical-sized calvarial defects in rats," *PLoS One* **13**(4), e0195337 (2018).
170. I. M. Zaccara et al., "Photobiomodulation therapy improves multilineage differentiation of dental pulp stem cells in three-dimensional culture model," *J. Biomed. Opt.* **23**(9), 095001 (2018).
171. S. Rochkind et al., "Increase of neuronal sprouting and migration using 780 nm laser phototherapy as procedure for cell therapy," *Lasers Surg. Med.* **41**(4), 277–281 (2009).
172. W. Zhu et al., "3D printing scaffold coupled with low level light therapy for neural tissue regeneration," *Biofabrication* **9**(2), 025002 (2017).
173. C. C. Shen et al., "Neural regeneration in a novel nerve conduit across a large gap of the transected sciatic nerve in rats with low-level laser phototherapy," *J. Biomed. Mater. Res. - Part A* **101**(10), 2763–2777 (2013).
174. S. H. Hsu et al., "The effect of laser preexposure on seeding endothelial cells to a biomaterial surface," *Photomed. Laser Surg.* **28**(SUPPL. 2), S37–S44 (2010).
175. H. El Nawam et al., "Low-level laser therapy affects dentinogenesis and angiogenesis of in vitro 3D cultures of dentin-pulp complex," *Lasers Med. Sci.* **34**(8), 1689–1698 (2019).
176. A. Gupta et al., "Superpulsed (Ga-As, 904 nm) low-level laser therapy (LLLT) attenuates inflammatory response and enhances healing of burn wounds," *J. Biophotonics* **8**(6), 489–501 (2015).
177. V. Cury et al., "Low level laser therapy reduces acute lung inflammation without impairing lung function," *J. Biophotonics* **9**(11–12), 1199–1207 (2016).
178. J. L. Costa Carvalho et al., "The chemokines secretion and the oxidative stress are targets of low-level laser therapy in allergic lung inflammation," *J. Biophotonics* **9**(11–12), 1208–1221 (2016).
179. R. A. Brochetti et al., "Photobiomodulation therapy improves both inflammatory and fibrotic parameters in experimental model of lung fibrosis in mice," *Lasers Med. Sci.* **32**(8), 1825–1834 (2017).
180. N. H. C. Souza et al., "Photobiomodulation and different macrophages phenotypes during muscle tissue repair," *J. Cell Mol. Med.* **22**(10), 4922–4934 (2018).
181. N. J. Prindeze et al., "Photobiomodulation elicits a differential cytokine response in a cultured analogue of human skin," *Eplasty* **19**, e3 (2019).
182. K. Shanmugapriya et al., "Multifunctional heteropolysaccharide hydrogel under photobiomodulation for accelerated wound regeneration," *Ceram. Int.* **46**(6), 7268–7278 (2019).
183. A. C. M. Renno et al., "Effect of 830 nm laser phototherapy on osteoblasts grown in vitro on Biosilicate® scaffolds," *Photomed. Laser Surg.* **28**(1), 131–133 (2010).
184. R. Fekrazad et al., "Effects of photobiomodulation and mesenchymal stem cells on articular cartilage defects in a Rabbit model," *Photomed. Laser Surg.* **34**(11), 543–549 (2016).
185. I. M. I. Zurina et al., "2D/3D buccal epithelial cell self-assembling as a tool for cell phenotype maintenance and fabrication of multilayered epithelial linings in vitro," *Biomed. Mater.* **13**(5), 054104 (2018).
186. I. M. Zurina et al., "Tissue engineering using a combined cell sheet technology and scaffolding approach," *Acta Biomater.* **113**, 63–83 (2020).
187. Y. M. Efremov et al., "Mechanical properties of cell sheets and spheroids: the link between single cells and complex tissues," *Biophys. Rev.* **13**(4), 541–561 (2021).
188. A. Shpichka et al., "Organoids in modelling infectious diseases," *Drug Discov. Today* **27**(1), 223–233 (2022).
189. P. R. Garrido et al., "Effects of photobiomodulation therapy on the extracellular matrix of human dental pulp cell sheets," *J. Photochem. Photobiol. B Biol.* **194**, 149–157 (2019).
190. A. C. F. Pedroni et al., "Photobiomodulation therapy and vitamin C on longevity of cell sheets of human dental pulp stem cells," *J. Cell Physiol.* **233**(10), 7026–7035 (2018).

191. S. Y. Chang et al., “Enhanced inner-ear organoid formation from mouse embryonic stem cells by photobiomodulation,” *Mol. Ther. - Methods Clin. Dev.* **17**, 556–567 (2020).
192. M. M. Marques et al., “Photobiomodulation of dental derived mesenchymal stem cells: a systematic review,” *Photomed. Laser Surg.* **34**(11), 500–508 (2016).

**Polina Bikmulina** received her bachelor’s and master’s degrees in biology from Lomonosov Moscow State University, Faculty of Biology, Russia, in 2019 and 2021. Currently, she is a PhD student at Sechenov University, Moscow, Russia. Since 2020, she has been a junior researcher at the Center «Digital Biodesign and Personalized Healthcare», Sechenov University, Moscow, Russia.

**Nastasia Kosheleva** received her specialist degree in physiology in 2003 from Lomonosov Moscow State University, Faculty of Biology. In 2007, she received her PhD in developmental biology, embryology. From 2007 to 2020, she has worked at Lomonosov Moscow State University. Currently, she is a leading researcher at the Center «Digital Biodesign and Personalized Healthcare», Sechenov University, and at the Institute of General Pathology and Pathophysiology, Laboratory of Cell Biology and Developmental Pathology, Moscow, Russia.

**Anastasia Shpichka** graduated from Penza State University, majoring in pharmacy. In 2013, she received her PhD in biotechnology from the Lomonosov Moscow State University. Currently, she is a leading researcher at the Laboratory of Clinical Smart Nanotechnologies, Sechenov University, Moscow, Russia.

**Vladimir Yusupov** graduated from the Moscow Institute of Physics and Technology and received his PhD in 2007. He studied the effects of laser light on biological objects and laser medicine. He is the author of more than 350 publications and 50 patents. Currently, he is a senior researcher at the Institute of Photon Technologies of RAS.

**Vladimir Gogvadze** obtained his specialist degree in physics from Tbilisi State University in 1973 and his PhD in biology from the Institute of Biological Physics, Pushchino, Russia, in 1984. Currently, he is an associate professor at Karolinska Institutet, Stockholm, Sweden. Since 2011, he has been a leading scientist at the Laboratory of Apoptosis Mechanism Investigation, Faculty of Medicine, Lomonosov Moscow State University, Russia. He is the author of more than 130 publications and three book chapters.

**Yury Rochev** obtained his specialist degree in physics from Lomonosov Moscow State University, Biophysical Department, Russia. In 1990, he was awarded a PhD in biophysics. He was appointed in biomedical engineering science at the National Centre for Biomedical Engineering Science, National University of Ireland, Galway, in 2007. He is the author of more than 120 journal papers and has written three book chapters.

**Peter Timashev** graduated from Lomonosov Moscow State University of Fine Chemical Technologies. He received his PhD (solid-state chemistry 2004) and his DSc degree in 2016 from Karpov Institute of Physical Chemistry. He is the head of the Biomedicine Science and Technology Park (Sechenov University, Moscow, Russia). He has authored more than 290 publications and 10 patents and is a laureate of the Moscow Government Prize.